Fermi National Accelerator Laboratory

FN-359
1500.000

SIMULATIONS OF THE BEAM-BEAM INTERACTION WITH TUNE MODULATION AT THE TEVATRON $p\bar{p}$ COLLIDER

D. Neuffer, A. Riddiford, and A. Ruggiero

February 1982

Operated by Universities Research Association Inc. under contract with the United States Department of Energy

Simulations of the Beam-Beam Interaction with Tune Modulation at the Tevatron $\bar{p}p$ Collider

D. Neuffer, A. Riddiford and A. Ruggiero

February 1982

Abstract

Simulations of weak-strong $\bar{p}p$ collisions with a periodic tune modulation show the possibility of beam blowup at sufficiently strong modulation amplitudes. This beam blowup is associated with the appearance of nonrepeatable "chaotic" trajectories and occurs when low order resonances are crossed by the modulation. The implication of this modulational beam blowup for beam-beam limitations and modulation amplitude limitations in $\bar{p}p$ colliders are discussed.

Introduction

In proton-antiproton ($p\bar{p}$) collisions in the "Tevatron"[1] particle trajectories will be affected by the highly nonlinear force of the "beam-beam" interaction, the electromagnetic force field of the opposite beam in the collisions. The trajectories between collisions will be subject to tune modulation from turn to turn through sources such as power supply ripple or synchrotron oscillations with uncorrected chromaticity. Previous investigations of the beam-beam interaction by the present authors[2,3,4,5] have considered a constant "beam-beam" interaction form and particle transport. In this paper we add the complication of tune modulation and investigate its effects.

We approximate particle circulation around the accelerator ring as the

product of two transformations; a linear transport around the storage ring followed by a nonlinear beam-beam "kick" at the interaction area.

Transport around the ring can be represented by a 2x2 matrix for both transverse (x and y) dimensions:

$$\begin{pmatrix} x \\ x' \end{pmatrix}_{\text{After}} = \begin{bmatrix} \cos 2\pi\nu_x & \beta_x \sin 2\pi\nu_x \\ -\dfrac{\sin 2\pi\nu_x}{\beta_x} & \cos 2\pi\nu_x \end{bmatrix} \begin{pmatrix} x \\ x' \end{pmatrix}_{\text{Before}} . \tag{1}$$

In this linear transport x and y motion are decoupled. ν_x, ν_y, β_x, β_y are the usual Courant-Snyder tunes and beta-functions. The beam-beam kick can be represented as

$$\begin{pmatrix} x \\ x' \end{pmatrix}_{\text{After}} = \begin{bmatrix} 1 & 0 \\ \dfrac{-4\pi\Delta\nu_x}{\beta_x} F_x(x,y) & 1 \end{bmatrix} \begin{pmatrix} x \\ x' \end{pmatrix}_{\text{Before}} \tag{2}$$

with a similar expression for y, y'.

The product of these transformations is equivalent to integration of the equation of motion:

$$x'' + K_x(s)x = -\frac{4\pi\Delta\nu_x}{\beta_x} F_x(x,y) \times \delta_p(s) \tag{3}$$

s, the distance along the storage ring, is the independent variable and $\delta_p(s)$ is a periodic delta-function.

In the present report we choose parameters which approximate the conditions[1] in the Tevatron: $\Delta\nu_x = \Delta\nu_y = 0.01$, $\beta_x = \beta_y = 2\,\text{m}$ and we choose

$$F_x = F_y = \frac{1-e^{-(x^2+y^2)/2\sigma^2}}{(x^2+y^2)/2\sigma^2} \tag{4}$$

with σ = 0.0816 mm which is the nonlinear force due to a round, gaussian charge distribution of rms radius σ. This nonlinear force function does not change from turn to turn which means that we use the "weak-strong" approximation where the "strong" beam is unaffected by the weak beam.

To simulate tune modulation, the tunes ν_x and ν_y in Equation (1) are changed from turn to turn following

$$\begin{aligned} \nu_x &= \nu_{x_0} + a_x \sin \omega_x t \\ \nu_y &= \nu_{y_0} + a_y \sin \omega_y t. \end{aligned} \tag{5}$$

We have used $\omega_x = \omega_y$ in all cases, which is expected for most reasonable sources of tune modulation and we have considered two possible relative phases:

$$a_y = a_x \text{ labelled ++} \tag{6}$$

and

$$a_y = -a_x \text{ labelled +-}.$$

The magnitudes of a_x and a_y are chosen as equal. We have chosen values of a_x between 0.001 and .01 = $\Delta\nu$, in agreement with expected values, in the present paper. For the frequency ω we have chosen a frequency precisely one thousandth (.001) of the collision frequency. Since the Tevatron collision frequency is 50 kHz, the modulation frequency is 50 Hz, quite close to expected power supply modulation (60 Hz) as well as the synchrotron motion frequency. The modulation is chosen as a precise fraction of the collision frequency to simplify computation; the matrix given by (1) can be calculated initially for each of the 1000 possible values and stored. This eliminates the necessity of recalculating (1) on each turn.

Possible Sources of Tune Modulation

One possible source of tune modulation is power supply ripple. Ripple in the power supplies of the focusing and defocusing quadrupoles will cause

a ripple in the tunes ν_x and ν_y. If there are separate focusing and defocusing quad supplies then we expect modulation of the $\pm$ type, if they are connected to the same supply, modulation of the $\mp$ kind. The modulation should occur at low order harmonics of 60 Hz. The amplitude of modulation is

$$\frac{\delta\nu}{\nu} \sim \frac{\delta G}{G} \sim \frac{\Delta I}{I} \tag{7}$$

where G is the magnetic gradient and I is the magnet current. With $\nu = 20$ and $\delta\nu = .001 - .01$, we find an equivalent power supply regulation $\frac{\delta I}{I} \sim 5 \times 10^{-5} - 5 \times 10^{-4}$; somewhat larger than that expected at the Tevatron.

Another possible cause of modulation is synchrotron oscillations coupled with uncorrected chromaticity. Synchrotron oscillations modulate particle momenta, following

$$\Delta p \sim \Delta p_o \sin(\nu_s r + \phi).$$

This leads to tune modulation of the form $(\mp)$

$$\begin{aligned} \delta\nu_x &\cong \nu_x \xi_x \frac{\Delta p_o}{p} \sin(\nu_s t + \phi) \\ \delta\nu_y &\cong \nu_y \xi_y \frac{\Delta p_o}{p} \sin(\nu_s t + \phi) . \end{aligned} \tag{8}$$

We expect $\frac{\Delta p}{p} \sim 10^{-4}$ in the Tevatron. ξ_x, ξ_y are the x and y chromaticities:

$$\xi_x = \frac{p}{\nu_x} \frac{\partial \nu_x}{\partial p} . \tag{9}$$

If chromaticity is uncorrected $\xi_x \cong \xi_y \cong -1$, The values of $\delta\nu(.001\text{-}.01)$ correspond to $|\xi| = (.5\text{-}5.)$ in the Tevatron. The chromaticity should be corrected to much less than 1 by sextupoles.

Thus the modulations expected in the Tevatron should be less than those explored in this note. (Other colliding beam machines (e^+e^-) do have larger tune modulations.) The relatively large values of this note are chosen to

find limits where large effects can occur.

Simulation Procedure

In the simulations a set of 100 initial particle positions are generated randomly within a gaussian distribution in the 4-D phase space (x,x',y,y'). These are transported through many turns following the transformations of Equations (1) and (2) with tunes modulated following Equation (5). Every 2000 turns the rms emittances X,Y, and R are calculated using:

$$X = 6\sqrt{\langle(x-\bar{x})^2\rangle \langle(x'-\bar{x}')^2\rangle}$$

$$Y = 6\sqrt{\langle(y-\bar{y})^2\rangle \langle(x'-\bar{x}')^2\rangle} \qquad (10)$$

$$R = \sqrt{X^2 + Y^2}$$

In these simulations 6 million turns (corresponding to 2 minutes Tevatron time) are calculated in each case, and 3000 emittance values are generated and analyzed statistically.

"Doubling" times for X,Y and R emittance are obtained from the slopes of the best straight line fits for X,Y and R as functions of time from t = 0, using rms emittance values calculated every 2000 turns.

The straight line fit of the x-emittance values can be written[6] as

$$X = \bar{X} + b(t-\bar{t}) \qquad (11)$$

where

$$\bar{X} = \frac{1}{N}\Sigma X_i \qquad (12)$$

$$\bar{t} = \frac{1}{N}\Sigma t_i \qquad (13)$$

$$b = \frac{1}{DEN}\left[\frac{1}{N}\Sigma X_i t_i - \bar{X}\,\bar{t}\right] . \qquad (14)$$

N is the total number of particles, and

$$DEN = \frac{1}{N}\Sigma t_i^2 - t^{-2} \tag{15}$$

$$SX^2 = \frac{1}{N-2}\Sigma\left[X_i - \bar{X} - b(t_i - \bar{t})\right]$$

$$= \frac{1}{1-2/N}\left[\frac{1}{N}\Sigma X_i^2 - X^2 + b^2\left(\frac{1}{N}\Sigma t_i^2 - t^{-2}\right)\right.$$

$$\left. - 2b\left(\frac{1}{N}\Sigma X_i t_i - \bar{X}\bar{t}\right)\right]. \tag{16}$$

The calculated slopes have a statistical error associated with the scattering of the points X_i, which is given by

$$\sigma_b^2 = \frac{SX^2}{N \cdot DEN} \cdot \tag{17}$$

A negative doubling time is obtained if b<0; that is, X is decreasing. In these simulations the calculated slopes are cumulative slopes, calculated by including all emittance values generated from t = 0 up to the measurement time.

Simulation Results

For our simulations of tune modulation we have chosen initial tunes at $\nu_x = .3439$, $\nu_y = .1772$, $\Delta\nu_{BB} = .01$. These are the parameters of Case C of Reference 3, which is a case chosen in a tune region free of resonances lower than ninth order and showed the greatest stability in the long-time simulations. The addition of tune modulation permits the appearance of low order resonances in combination with the modulation. Figure 1 shows the "tune-space" near the Case C tunes, and one finds third, sixth and eighth order resonances within $\delta\nu = .01$ of Case C and therefore accessible by tune modulation.

We have considered 13 separate modulation cases:

(1) $\delta\nu = 0$ (no modulation) which is Case C of Reference 3.

(2) (++) modulation with $\delta\nu_x = \delta\nu_y = .001, .003, .005, .007, .009, .01$.

(3) (+-) modulation with $\delta\nu_x = -\delta\nu_y = .001, .003, .004, .005, .007, .01$.

In Tables 1-3 and Figures 2-4 we present results of the (++) simulations with $\delta\nu = .003$, $\delta\nu = .007$, $\delta\nu = .010$. In each case we have simulated 6 million turns of beam storage. In Tables 4-7 and Figures 5-8 we present results of the (+-) simulations with $\delta\nu = .003$, .004, .005 and .010.

In the (++) simulations we saw no significant changes in the rms beam emittances for $\delta\nu \lesssim .009$. However, for $\delta\nu = .01$ some statistically significant changes appear. There is a strong anticorrelation between changes in x-emittance and changes in y-emittance, as can be seen in Figure 4 and the cumulative correlation coefficient of Table 3. There are also statistically significant changes in these rms emittances, but the changes are $\lesssim$1% after 6 million turns, and represent "doubling times" of $\gtrsim$0.1 days, only a few standard deviations from zero change.

For the (+-) simulations more dramatic changes occur. For $\delta\nu < .003$ no statistically significant changes occur but for $\delta\nu > .004$ there is a fast blowup of the beam emittances, with doubling times of fractions of a minute rather than days. The blowup is evident within 200,000 turns of particle motion and continues throughout the six million turn simulations.

Our tentative conclusion is that beam blowup can occur when there is tune modulation and beam-beam interaction, when the modulation is of adequate amplitude.

Repeatability Experiments

Our basic test of computational accuracy is a repeatability test. In these tests initial particle positions are transported forward N turns, the transport transformations are reversed and the particle trajectories are returned. Forward and return particle positions are compared. As we discussed in a previous paper[4] "chaotic" trajectories diverge exponentially in a repeatability test and the test is a useful tool for distinguishing these trajectories.

In Table 8 we summarize the results of repeatability tests for 11 tune modulation cases. In these, 100 trajectories are transported 100,000 turns forward and returned. Most trajectories develop errors of order 10^{-20} in agreement with the expected error for non-chaotic trajectories. However in the (+-) simulations large error trajectories appear for $\delta\nu > .004$; about 10/100 for $\delta\nu = .004$, and ~50/100 for $\delta\nu > .005$. In the (++) cases no large error trajectories appear until the largest $\delta\nu$ value (.01) where 3-6% are large error.

Following the analyses of Reference 4 we identify these large error trajectories as "chaotic" trajectories. There are some differences between this and the previous case of Reference 4. First, the division between "chaotic" and non-chaotic cases is not as clearly defined; some trajectories with small exponential divergence appear. Second, in this case the chaotic trajectories can diverge to large amplitudes.

We use a strong correlation between beam blowup and the appearance of chaotic trajectories, and we can infer that the appearance of chaotic trajectories is necessary for beam blowup.

Tune Modulation, Chaotic Trajectories, Resonances and Beam Blowup

In this section we undertake a more systematic discussion on the inter-relationships between the topics discussed above: tune modulation, beam blowup, low-order resonances and chaotic trajectories. As we mentioned above, the addition of tune modulations permits the appearance of low order resonances. In Figure 9 we show the tune diagram for (+-) $.005 = \delta\nu$, a case with beam blowup and ~40 chaotic trajectories. A box representing the tune spread of the beam ($\Delta\nu_x = \Delta\nu_y = .01$) is outlined at the center ($\delta\nu_x = \delta\nu_y = 0$) and at the extremes of the tune modulations ($\delta\nu_x = .005$, $\delta\nu_y = .005$ and $\delta\nu_x = .005$, $\delta\nu_y = .005$). The full extent of the modulation is outlined with a darkened line. Low order resonances of third, sixth and eighth orders are also indicated by darkened lines within the modulated beam tune spread.

(The other lines are higher order resonances.)

The appearance of chaotic trajectories in the (+-) simulations is definitely correlated with the inclusion of the third and sixth order resonances ($-\nu_x + 2\nu_y = 0$, $4\nu_x - 2\nu_y = 1$). This can be made more definite by considering the progression of (+-) cases $\delta\nu$ = .003, .004 and .005 (see Figures 5,6 and 7). At .003 the resonances barely intersect the edges of the tune modulation and do not affect the particle motion; there is no beam blow-up. At .004 the resonances do intersect the beam for large amplitude particle motions, we find 10% chaotic trajectories and beam blow-up. At $\delta\nu$ = .005 the resonance line intersects the center of the tune square at the extremes of the tune modulation; ~40 - 50% of the trajectories are chaotic.

In Figure 10 we show particle tunes averaged over the first thousand turns for the ±.005 case. These tunes are calculated by taking the differences in the phases

$$\phi_x = \text{ATAN}\left(\frac{\bar{\beta}x'}{x}\right)$$

$$\phi_y = \text{ATAN}\left(\frac{\bar{\beta}y'}{y}\right)$$

from turn to turn (see Figure 11). For $\bar{\beta}$ an amplitude dependent average between $\beta = \beta_o$ (at zero amplitude) and $\beta = \beta^*$ (the matrix β for ∞ amplitude) is used.

The tunes are concentrated near the diagonal $\Delta\nu_x = \Delta\nu_y$ as is expected from basic considerations.

The investigations of particle trajectories find that they can be categorized into three distinct groups.

1. "Non-chaotic" (repeatable) trajectories which do not change their mean amplitudes substantially in long-time simulations.

2. "Chaotic" trajectories which may undergo some change in mean amplitudes but do not diverge to large amplitudes.

3. "Chaotic" trajectories which do diverge to large amplitude.

In Figure 10 we have identified these three separate types and find that they occupy distinct regions in tune space. The largest amplitude particles (these are those with largest beam-beam tune shifts) are predominantly chaotic and divergent. Intermediate amplitude trajectories are chaotic but not divergent. Smaller amplitude particles are non-chaotic.

This separation is in agreement with an intuitive picture in which chaotic trajectories are caused by sweeping of a low order resonance through the beam, and only those trajectories which reach an amplitude swept by the resonance can be chaotic.

This picture is confirmed by consideration of the (+-) .004 case. The nine chaotic, divergent trajectories are among the largest amplitude divergent trajectories of the (+-) .005 case and are consistent with the observation that the lower amplitude of tune modulation should only "sweep" through the largest amplitude particles. These largest amplitude particles are also labeled in Figure 10.

We have also confirmed the hypothesis that tune modulation is necessary for the appearance of chaotic, divergent trajectories. We have undertaken six million turn simulations at the center (ν_x = .3439, ν_y = .1772, $\Delta\nu$ = .01) and at the two extremes of the tune modulation, (ν_x = .3489, ν_y = .1722, $\Delta\nu$ = .01) and (ν_x = .3389, ν_y = .1822, $\Delta\nu$ = .01) without modulation. No chaotic trajectories and no beam blow-up are seen, even though the extremes do contain third or sixth order resonances.

Discussion of Chaotic Trajectories for (++) Simluations

For the (++) simulations only the largest amplitude case shows evidence of chaotic trajectories and it shows no large beam blow-up ($\delta\nu$ = .01). In Figure 12 we show the tune diagram for the .01 modulation case and this shows a few low order resonances within the modulation amplitude.

Investigation of particle amplitudes indicates that the sixth and third order resonances in the lower right of the tune diagram are probably associated with these chaotic trajectories. Only largest amplitude particles which could reach these resonances are chaotic; and these would not reach them at a lower modulation amplitude. Since only a few particles can reach these resonances and even these do not cross them at significant speeds, there is no beam blow-up in this case.

Conclusions

Simulations of the beam-beam interaction with tune modulation find that beam blow-up can occur if the modulation sweeps the beam through a low order ($\lesssim$8th order) resonance. Modulations $\gtrsim$.01 would be forbidden by this criterion with a beam-beam tune shift of $\gtrsim$.01, since it is difficult to find a region free of low order resonances. No beam blow-up should occur at the lower amplitude modulations expected at the Tevatron.

References

1. Tevatron I Design Report, Fermilab, May 1981

2. D. Neuffer, A. Riddiford and A. Ruggiero, FN-333, April 1981

3. D. Neuffer, A. Riddiford and A. Ruggiero, FN-343, July 1981

4. D. Neuffer, A. Riddiford and A. Ruggiero, FN-346, October 1981

5. D. Neuffer, A. Riddiford and A. Ruggiero

6. P.K. Bevington, Data Reduction and Error Analysis for the Physical Sciences, McGraw-Hill, New York, 1969

TABLE 1 Emittance data Case C+.003 $\nu_x = 0.3439 + 0.003\sin\theta$ $\theta = 2\pi(n-1)/1000$

Cumulative values. $\nu_y = 0.1772 + 0.003\sin\theta$ n = turn number

$\Delta\nu = 0.01$

Million Turns	Doubling Time-X (days)	Doubling Time-Y (days)	Doubling Time-R (days)	Correlation Coefficient Bar Average	Correlation Coefficient Cumulative
0.2	(±0.0122)	(±0.0110)	(±0.0165)		
0.2	0.0240	0.0135	0.0169	-0.025	-0.025
0.4	-0.0425	-0.0741	-0.0567	-0.126	-0.089
0.6	-0.162	0.166	0.562	0.002	-0.062
0.8	0.665	0.109	0.179	-0.013	-0.049
1.0	0.235	0.0750	0.111	-0.080	-0.053
1.2	0.286	0.173	0.215	0.085	-0.033
1.4	-0.824	-0.455	-0.578	-0.101	-0.044
1.6	-0.592	-0.195	-0.286	0.009	-0.035
1.8	-0.855	-0.281	-0.411	0.094	-0.021
2.0	-0.443	-0.607	-0.517	0.114	-0.009
2.2	-0.312	1.04	-1.01	0.031	-0.007
2.4	-0.206	0.630	-0.709	-0.171	-0.022
2.6	-0.221	0.479	-1.01	-0.125	-0.031
2.8	-0.276	0.583	-1.30	0.027	-0.027
3.0	-0.446	0.622	-5.38	0.008	-0.025
3.2	-1.15	0.842	4.51	0.148	-0.015
3.4	-8.66	1.07	2.30	0.104	-0.009
3.6	-5.44	0.647	1.37	-0.056	-0.012
3.8	91.6	0.658	1.24	-0.099	-0.016
4.0	1.47	0.735	0.965	-0.103	-0.019
4.2	1.20	0.775	0.937	-0.069	-0.021
4.4	1.81	0.677	0.965	0.021	-0.019
4.6	5.98	0.978	1.63	0.078	-0.015
4.8	-3.71	1.64	5.31	0.203	-0.006
5.0	-2.00	2.16	342.	0.064	-0.003
5.2	-2.11	61.8	-4.55	-0.121	-0.008
5.4	9.58	3.06	4.68	0.006	-0.006
5.6	2.52	2.47	2.55	-0.025	-0.007
5.8	1.56	2.32	1.92	-0.040	-0.007
6.0	1.23	2.68	1.76	0.182	-0.001
6.0	(±1.77)	(±1.66)	(±2.41)		

TABLE 2 Emittance data for Case C+.007: $\nu_x = 0.3439 + 0.007 \sin\theta$ $\theta = 2\pi(n-1)/1000$

$\nu_y = 0.1772 + 0.007 \sin\theta$ n = turn number

$\Delta\nu = 0.01$

Million Turns	X Average (mm-mrad)	Doubling Time-X (days)	Y Average (mm-mrad)	Doubling Time-Y (days)	R Average (mm-mrad)	Doubling Time-R (days)	Correlation Coefficient Bar Average	Correlation Coefficient Cumulative
0.2		(±0.0111)		(±0.0114)		(±0.0159)		
0.2	0.0175451	0.0675	0.0187678	0.0430	0.0256926	0.0513	0.003	0.0026
1.0	0.0175494	-1.3	0.0187952	0.112	0.0257155	0.225	-0.027	0.0344
2.0	0.0175418	-0.361	0.0188039	0.177	0.0257168	0.0573	-0.059	0.0204
3.0	0.0175440	-2.79	0.0187994	3.30	0.0257151	49.1	-0.170	0.0165
4.0	0.0175370	-0.595	0.0188046	0.700	0.0257141	-736.	-0.119	0.0062
5.0	0.0175384	-1.92	0.0188024	3.38	0.0257134	-13.4	0.113	0.0015
5.2	0.0175400	-25.4	0.0188008	-7.57	0.0257134	-12.3	0.015	0.0008
5.4	0.0175413	3.18	0.0188021	4.88	0.0257152	3.81	-0.233	-0.0046
5.6	0.0175411	4.29	0.0188042	1.50	0.0257166	2.13	0.012	-0.0043
5.8	0.0175415	3.11	0.0188033	2.52	0.0257162	2.74	0.122	-0.0008
6.0	0.0175418	2.87	0.0188036	2.34	0.0257166	2.55	-0.096	-0.0030
6.0		(±1.81)		(±1.64)		(±2.43)		

TABLE 3 Emittance data for Case C+.010: $\nu_x = 0.3439 + 0.010 \sin\theta$ $\theta = 2\pi(n-1)/1000$

$\nu_y = 0.1772 + 0.010 \sin\theta$ n = turn number

$\Delta\nu = 0.01$

Million Turns	X Average (mm-mrad)	Doubling Time-X (days)	Y Average (mm-mrad)	Doubling Time-Y (days)	R Average (mm-mrad)	Doubling Time-R (days)	Correlation Coefficient Bar Average	Correlation Coefficient Cumulative
0.2		(±0.0129)		(±0.0104)		(±0.0172)		
0.2	0.0174482	-0.00679	0.0189352	0.00912	0.0257479	-0.115	-0.172	-0.172
1.0	0.0174502	0.0248	0.0188071	-0.0100	0.0256575	-0.0289	-0.084	-0.319
2.0	0.0174321	-0.0639	0.0187847	2.84	0.0256291	-0.145	-0.067	-0.385
3.0	0.0173396	-0.0286	0.0189546	0.0190	0.0256926	0.0778	-0.361	-0.540
4.0	0.0173504	-0.0854	0.0189498	0.0484	0.0256959	0.170	-0.069	-0.476
5.0	0.0173539	-0.175	0.0189573	0.0786	0.0257036	0.234	-0.173	-0.448
5.2	0.0173511	-0.171	0.0189625	0.0794	0.0257055	0.241	-0.200	-0.444
5.4	0.0173497	-0.179	0.0189655	0.0835	0.0257068	0.255	-0.232	-0.439
5.6	0.0173558	-0.292	0.0189563	0.117	0.0257041	0.327	-0.070	-0.440
5.8	0.0173615	-0.596	0.0189473	0.177	0.0257013	0.439	-0.033	-0.440
6.0	0.0173697	2.18	0.0189343	0.445	0.0256974	0.705	-0.184	-0.453
6.0		(±1.47)		(±1.14)		(±2.31)		

TABLE 4 Emittance data Case C-.003 $\nu_x = 0.3439 + 0.003\sin\vartheta$ $\vartheta = 2\pi(n-1)/1000$

Cumulative values. $\nu_y = 0.1772 - 0.003\sin\vartheta$ n = turn number

$\Delta\nu = 0.01$

Million Turns	Doubling Time-X (days)	Doubling Time-Y (days)	Doubling Time-R (days)	Correlation Coefficient Bar Average	Correlation Coefficient Cumulative
0.2	(±0.0112)	(±0.00933)	(±0.0145)		
0.2	0.0290	-0.0150	-0.0523	-0.049	-0.049
0.4	-0.0426	0.0193	0.0592	0.042	-0.006
0.6	0.131	0.105	0.116	0.040	0.007
0.8	0.0625	1.11	0.131	-0.028	-0.004
1.0	0.0587	0.0947	0.0740	-0.089	-0.012
1.2	0.126	0.230	0.166	-0.225	-0.044
1.4	0.204	0.341	0.261	0.004	-0.038
1.6	0.422	0.226	0.291	0.050	-0.028
1.8	-0.406	0.638	-3.17	-0.070	-0.031
2.0	-0.268	1.07	-0.809	0.040	-0.022
2.2	-0.443	1.41	-1.51	0.013	-0.019
2.4	-0.584	0.421	2.17	0.175	-0.007
2.6	-0.533	0.425	2.66	0.034	-0.004
2.8	-1.54	0.815	2.88	0.138	-0.007
3.0	-4.28	0.788	1.74	-0.085	-0.0005
3.2	1.19	0.679	0.847	0.029	0.002
3.4	0.978	0.998	0.985	-0.072	-0.003
3.6	0.828	8.05	1.58	-0.010	-0.004
3.8	0.741	1.75	1.07	0.307	0.011
4.0	0.811	2.35	1.25	0.083	0.014
4.2	0.731	1.90	1.09	0.202	0.023
4.4	0.505	1.12	0.717	0.099	0.027
4.6	0.704	0.982	0.831	-0.151	0.019
4.8	1.09	1.52	1.29	0.105	0.023
5.0	0.962	1.14	1.05	0.020	0.023
5.2	0.838	1.60	1.12	0.060	0.024
5.4	0.857	2.36	1.30	0.028	0.024
5.6	0.711	3.04	1.20	0.008	0.024
5.8	0.739	36.7	1.55	0.092	0.026
6.0	0.766	-103.	1.65	-0.017	0.025
6.0	(±1.71)	(±1.66)	(±2.35)		

TABLE 5 Emittance data for Case C-.004: $\nu_x = 0.3439 + 0.004 \sin\theta$ $\theta = 2\pi (n-1)/1000$

$\nu_y = 0.1772 - 0.004 \sin\theta$ n = turn number

$\Delta\nu = 0.01$

Million Turns	X Average (mm-mrad)	Doubling Time-X (minutes)	Y Average (mm-mrad)	Doubling Time-Y (minutes)	R Average (mm-mrad)	Doubling Time-R (minutes)	Correlation Coefficient Bar Average	Correlation Coefficient Cumulative
0.2		(±3.24)		(±4.74)		(±7.43)		
0.2	0.0178009	0.409	0.0196967	3.89	0.0265777	0.782	-0.314	-0.314
1.0	0.0272806	0.366	0.0227469	2.40	0.0360013	0.557	-0.672	-0.101
2.0	0.0309307	1.33	0.0253042	1.24	0.0406852	1.26	-0.570	-0.118
3.0	0.0322477	2.48	0.0327815	0.942	0.0469281	1.36	-0.639	+0.116
4.0	0.0337890	3.05	0.0358257	1.42	0.0500670	1.96	-0.530	+0.207
5.0	0.0354156	3.38	0.0400501	1.56	0.0542889	2.10	-0.662	0.367
5.2	0.0358952	3.30	0.0411124	1.56	0.0554246	2.07	-0.764	0.398
5.4	0.0365291	3.11	0.0425069	1.51	0.0569123	1.99	-0.706	0.468
5.6	0.0371243	3.00	0.0436633	1.51	0.0581714	1.96	-0.644	0.518
5.8	0.0376764	2.94	0.0447627	1.53	0.0593655	1.96	-0.569	0.552
6.0	0.0381485	2.95	0.0458627	1.56	0.0605107	1.97	-0.104	0.581
6.0		(±187.)		(±164.)		(±266.)		

TABLE 6 Emittance data for Case C-.005: $\nu_x = 0.3439 + 0.005 \sin\theta$ $\theta = 2\pi(n-1)/1000$

Cumulative values. $\nu_y = 0.1772 - 0.005 \sin\theta$ n = turn number

$\Delta\nu = 0.01$

Million Turns	X Average (mm-mrad)	Doubling Time-X (minutes)	Y Average (mm-mrad)	Doubling Time-Y (minutes)	R Average (mm-mrad)	Doubling Time-R (minutes)	Correlation Coefficient Bar Average	Correlation Coefficient Cumulative
0.2		($\pm$1.73)		($\pm$1.56)		($\pm$4.29)		
0.2	0.0312934	0.096	0.0318081	0.072	0.0448839	0.082	0.647	0.647
1.0	0.0641678	0.324	0.0550302	0.393	0.0850926	0.351	-0.706	0.706
2.0	0.0857574	0.608	0.0715130	0.719	0.1121701	0.652	-0.265	0.820
3.0	0.1074731	0.827	0.0893808	0.861	0.1403270	0.834	-0.787	0.872
4.0	0.1201061	1.20	0.1040974	1.11	0.1595478	1.16	-0.520	0.869
5.0	0.1341416	1.47	0.1151100	1.44	0.1773397	1.45	-0.614	0.888
5.2	0.1357520	1.57	0.1173479	1.50	0.1800303	1.54	-0.679	0.886
5.4	0.1377507	1.64	0.1194487	1.56	0.1829188	1.61	-0.703	0.887
5.6	0.1401047	1.70	0.1217876	1.60	0.1862225	1.66	-0.616	0.892
5.8	0.1424634	1.76	0.1246252	1.61	0.1898706	1.70	-0.525	0.896
6.0	0.1448834	1.80	0.1276645	1.63	0.1937078	1.73	-0.652	0.899
6.0		($\pm$255.)		($\pm$311.)		($\pm$374.)		

TABLE 7 Emittance data for Case C-.010: $\nu_x = 0.3439 + 0.010 \sin\theta$ $\theta = 2\pi(n-1)/1000$

$\nu_y = 0.1772 - 0.010 \sin\theta$ n = turn number

$\Delta\nu = 0.010$

Million Turns	X Average (mm-mrad)	Doubling Time-X (minutes)	Y Average (mm-mrad)	Doubling Time-Y (minutes)	R Average (mm-mrad)	Doubling Time-R (minutes)	Correlation Coefficient Bar Average	Correlation Coefficient Cumulative
0.2		(±3.48)		(±3.72)		(±5.79)		
0.2	0.0220899	0.131	0.0203253	0.370	0.0300772	0.186	0.590	0.590
1.0	0.0395563	0.310	0.0370738	0.274	0.0544489	0.291	-0.558	0.839
2.0	0.0491526	0.772	0.0710811	0.350	0.0877118	0.429	-0.280	0.790
3.0	0.0679651	0.667	0.1027513	0.527	0.1242134	0.572	-0.568	0.895
4.0	0.0986038	0.649	0.1315055	0.716	0.1655659	0.696	0.170	0.914
5.0	0.1356766	0.733	0.1554637	0.956	0.2083694	0.850	-0.298	0.910
5.2	0.1415717	0.769	0.1609772	0.988	0.2163504	0.884	0.309	0.918
5.4	0.1484026	0.796	0.1676349	1.00	0.2258152	0.907	0.170	0.928
5.6	0.1542386	0.832	0.1754262	1.01	0.2354864	0.930	-0.542	0.926
5.8	0.1588753	0.880	0.1835314	1.02	0.2446775	0.958	-0.204	0.916
6.0	0.1632004	0.929	0.1920187	1.02	0.2540140	0.985	0.187	0.906
6.0		(±187.)		(±220.)		(±399.)		

TABLE 7

TABLE 8 Summary of reversibility tests (100,000 turns forward; 100,000 turns back) for the 100 particles of cases C ± A: $\nu_x = 0.3439 + A \sin\theta$ $\theta = 2\pi(n-1)/1000$

$\nu_y = 0.1772 \pm A \sin\theta$ n = turn number

$\Delta\nu = 0.010$

Integer part of error $\log_{10}\sqrt{(\Delta x)^2 + (\Delta y)^2 + (\beta_x \Delta x')^2 + (\beta_y \Delta y')^2}$

Case	<-10	-10	-11	-12	-13	-14	-15	-16	-17	-18	-19	-20	-21	-22
C-.001												90	9	1
C-.003												90	9	1
C-.004	9				1	1			1	1	1	76	9	1
C-.005	38					1			1	1	3	45	10	1
C-.010	31	1	2	2			4	3	1	3	3	34	14	2
									(<-4)	(-4)	(-5)	(-6)	(-7)	(-8)
C-.010	SINGLE PRECISION								45	2	2	32	16	3
C+.001												90	9	1
C+.003												90	9	1
C+.005												90	9	1
C+.007						1						89	9	1
C+.009						1					2	87	9	1
C+.010	3					1		1	1			84	9	1
									(<-4)	(-4)	(-5)	(-6)	(-7)	(-8)
C+.010	SINGLE PRECISION								6			81	12	1

TABLE 8

Figure Captions

Figure 1 Tune region near case C

Figure 2 Results of (++ .003) Simulation

Figure 3 Results of (++ .007) simulation

Figure 4 Results of (++ .010) simulation

Figure 5 Results of (+- .003) simulation

Figure 6 Results of (+- .004) simulation

Figure 7 Results of (+- .005) simulation

Figure 8 Results of (+- .010) simulation

Figure 9 Tune region of (+- .005)

Figure 10 Particle tunes averaged over the first 1000 turns for case C ±.005)

Figure 11 Calculation of individual particle tune shifts

Figure 12 Tune Region of (++ .010)

Figure **1** Tune space showing the limits of Case C and how close the corners come to the undesirable lines of order 3, 6 and 8.

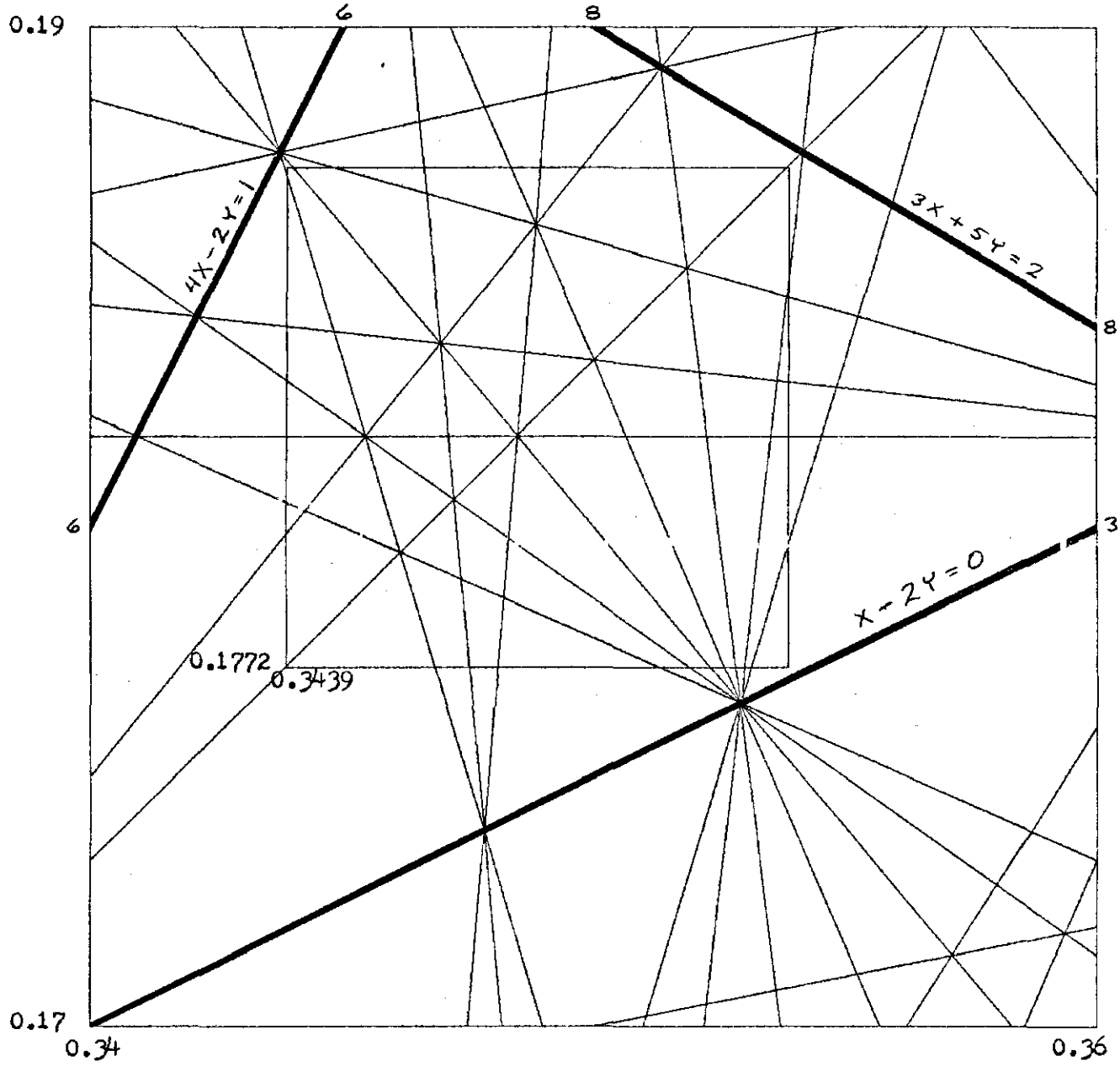

Fig. 2 Results of (++ .003) Simulation

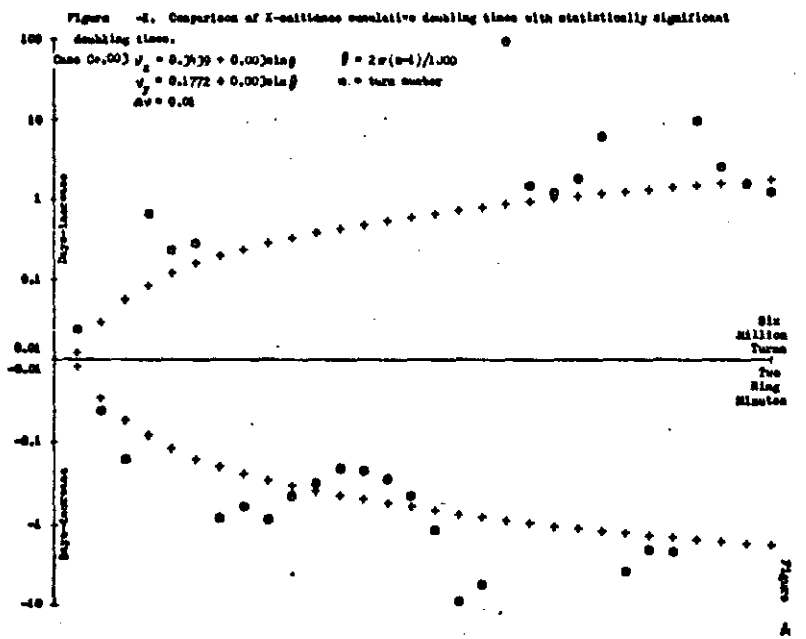

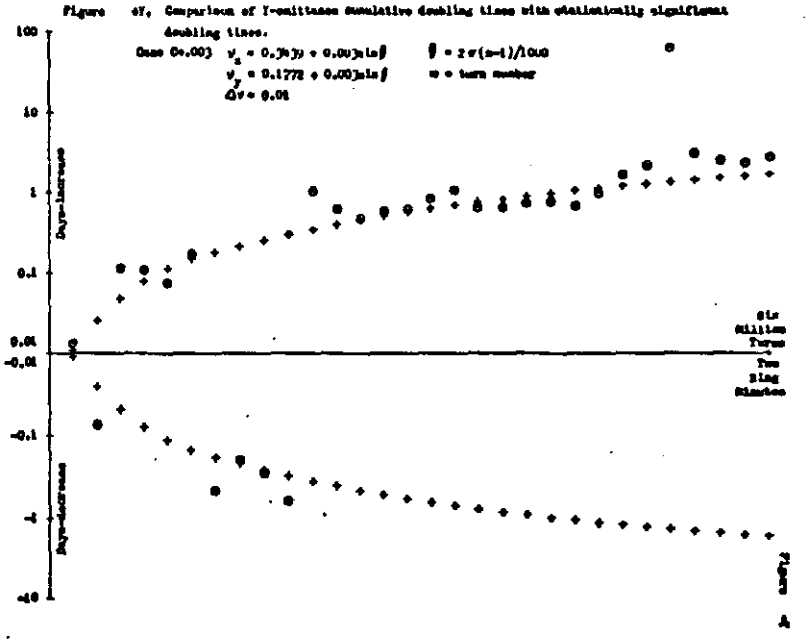

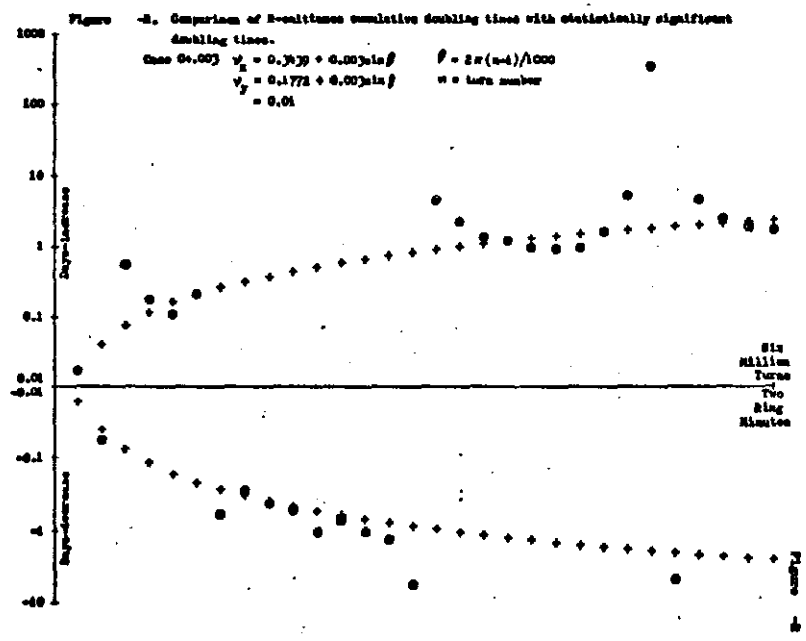

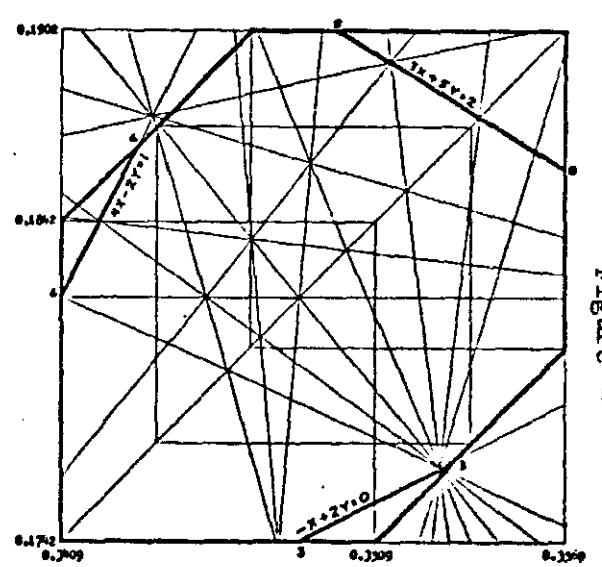

Figure 2

Fig. 3 Results of (++.007) simulation

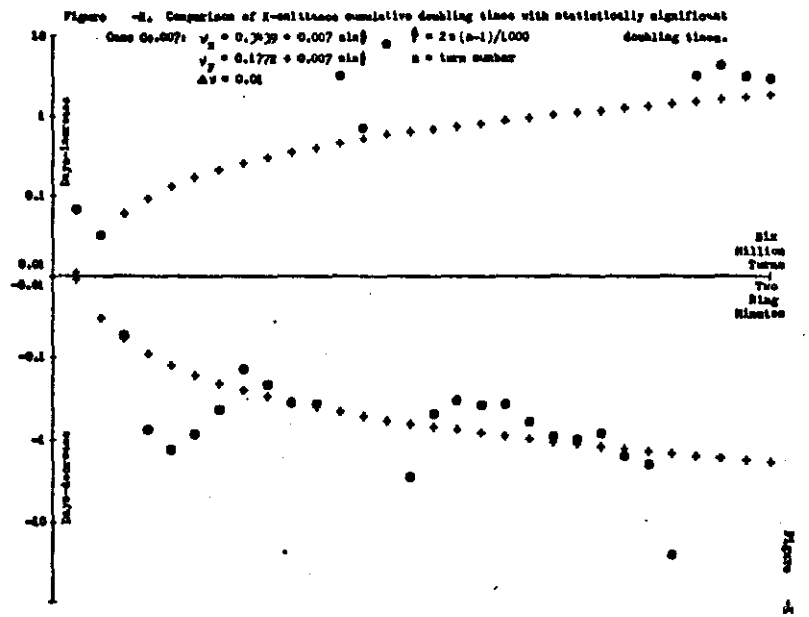

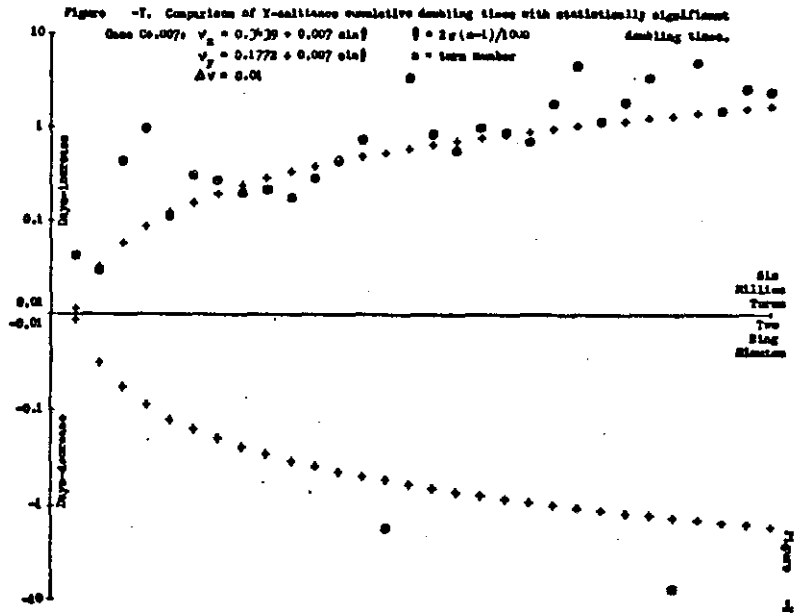

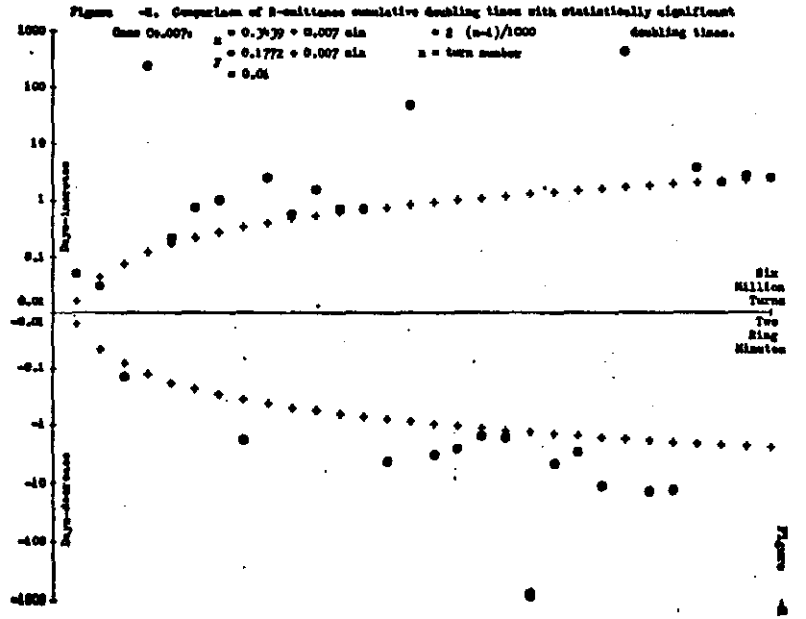

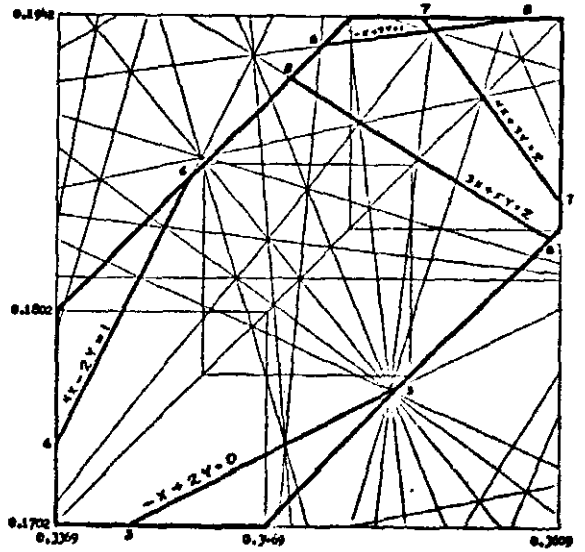

Figure 3

Fig. 4 Results of (++ .010) simulation

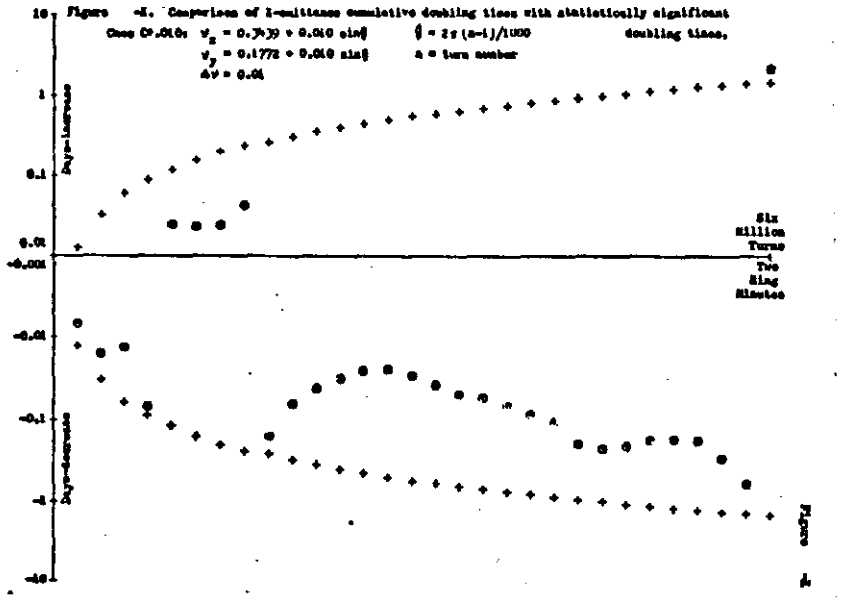

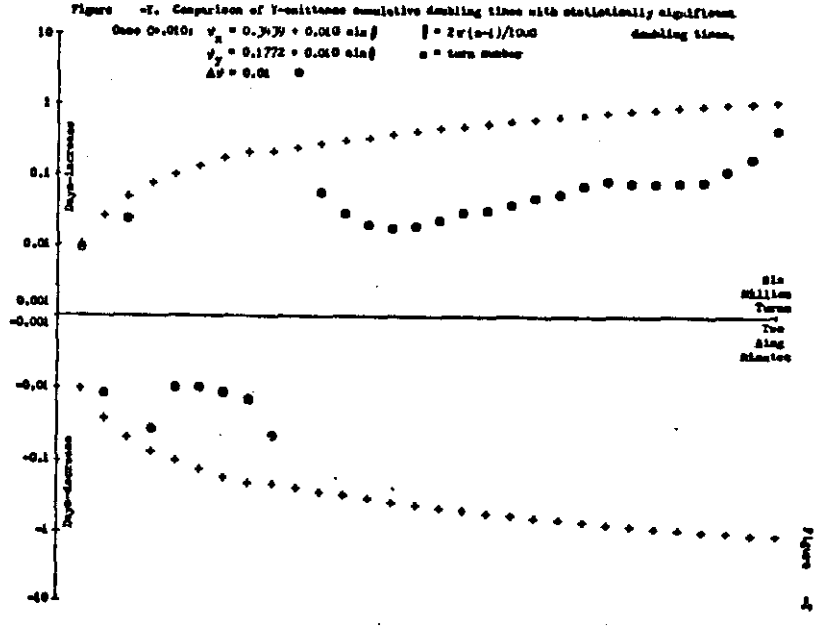

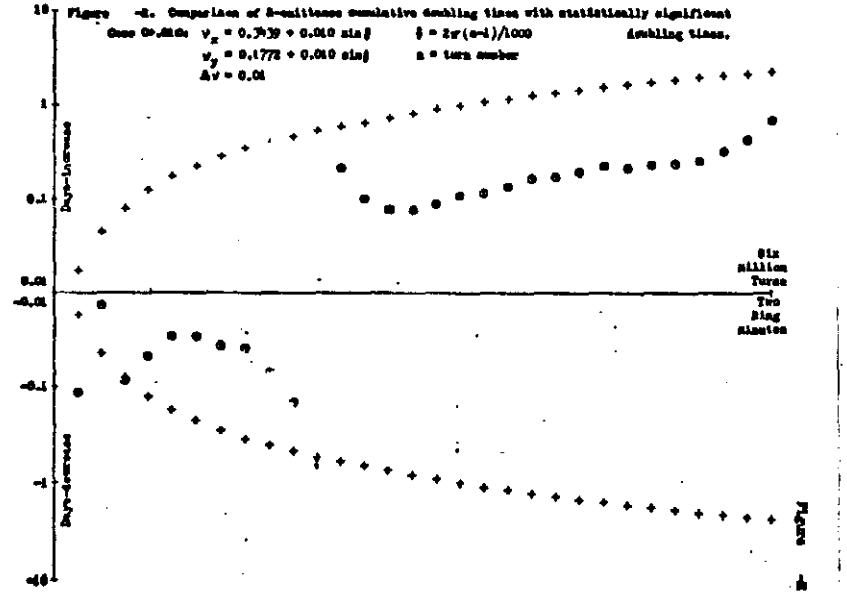

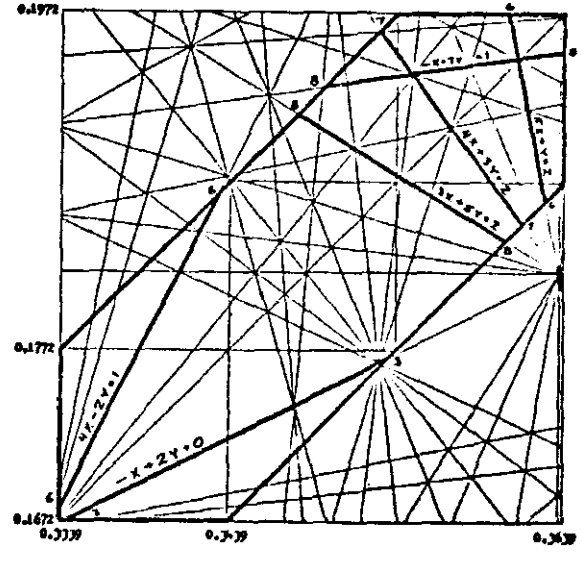

Figure 4

Fig. 5 Results of (+- .003) Simulation

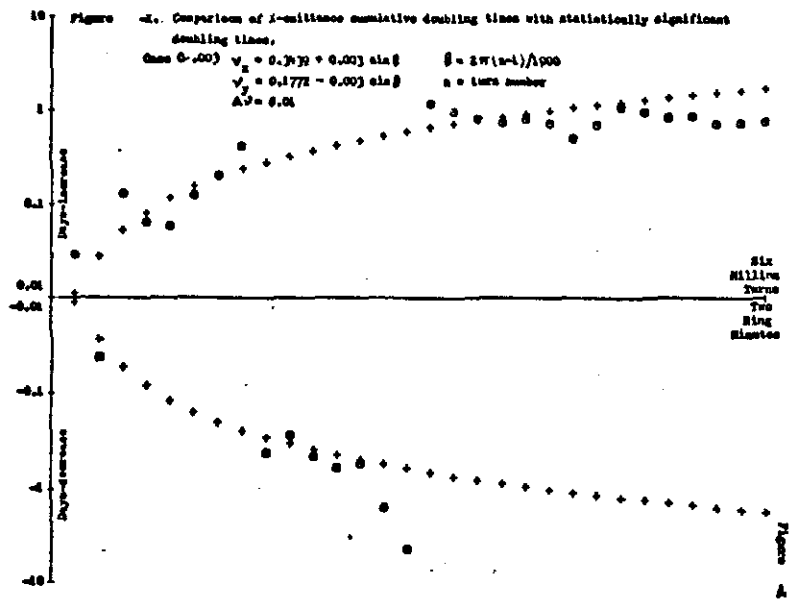

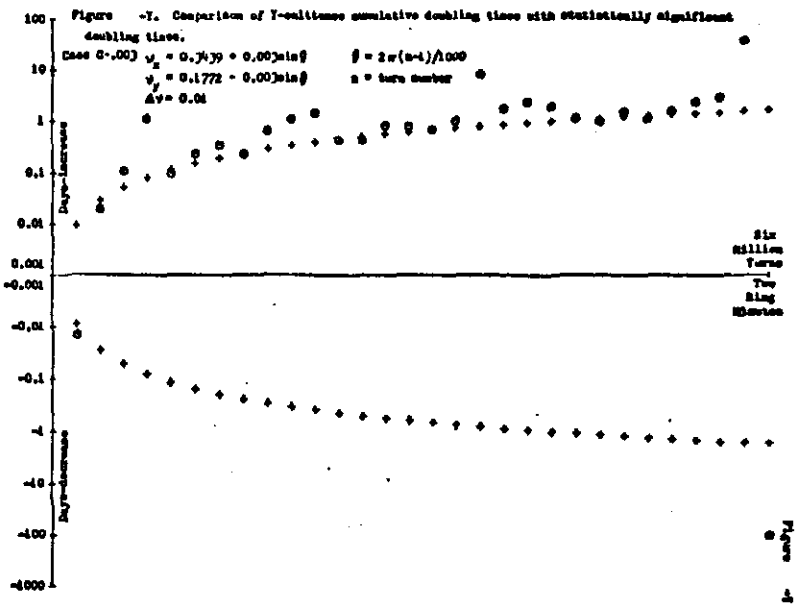

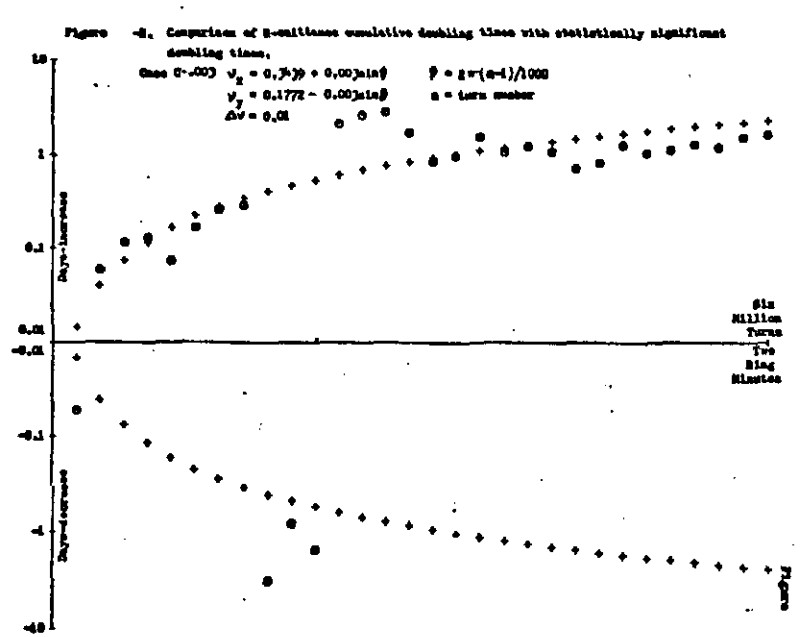

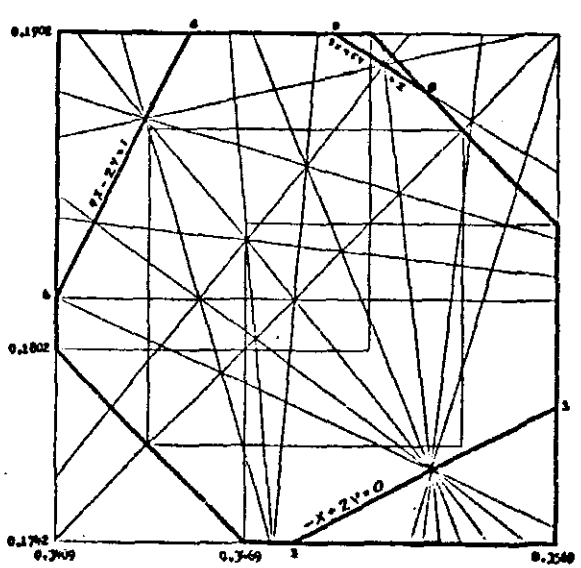

Figure 5

Fig. 6 Results of (+- .004) simulation

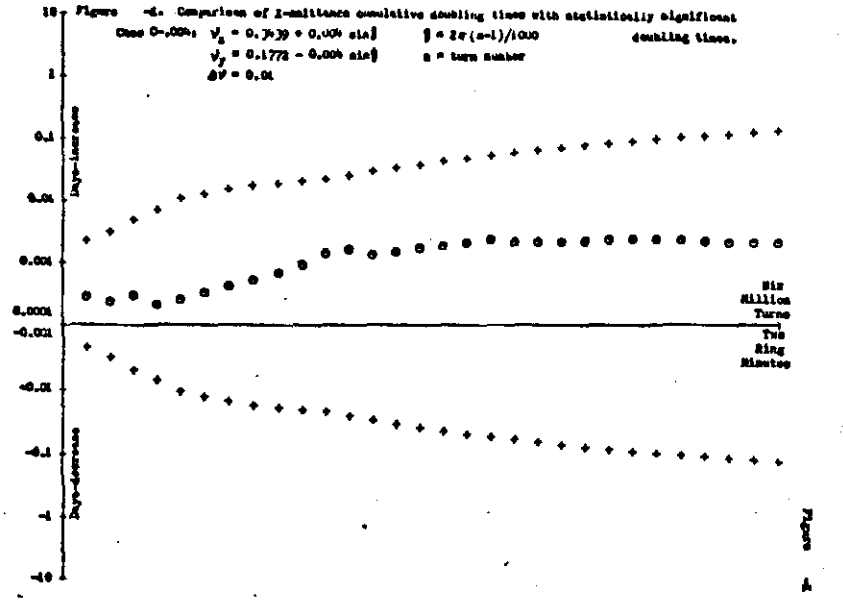

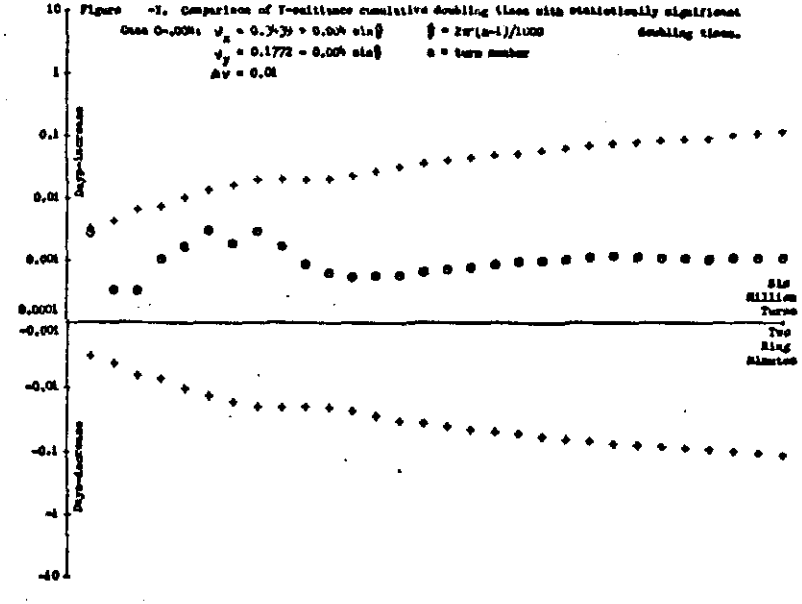

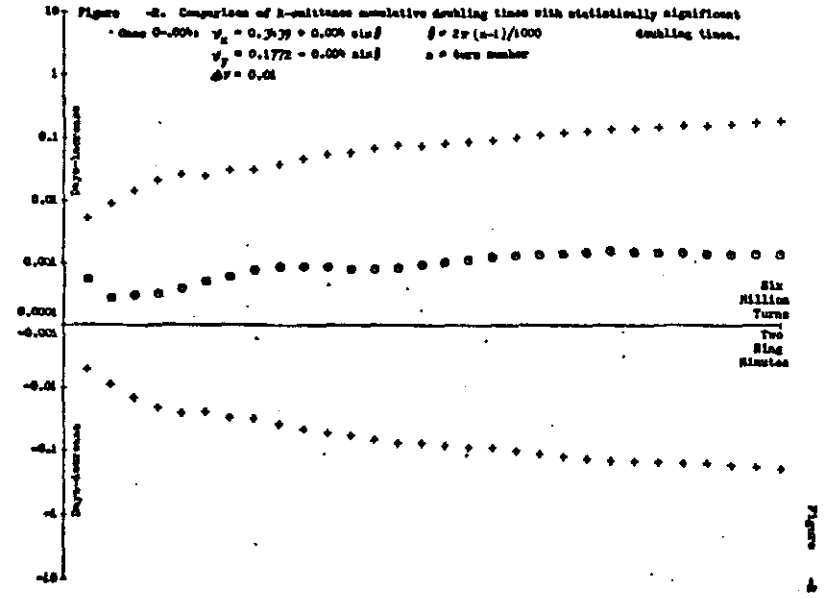

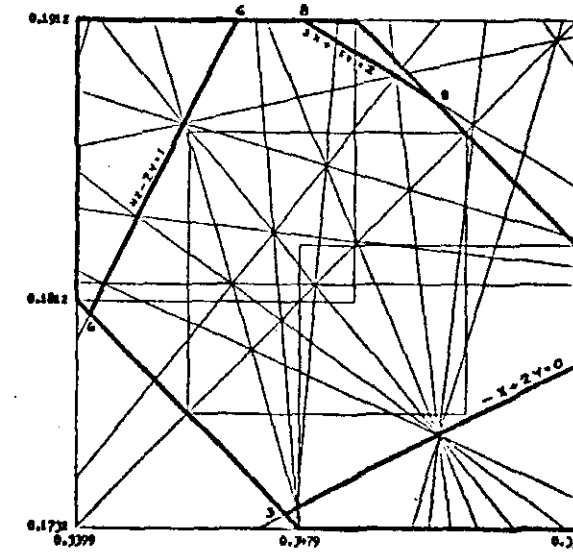

Figure 6

Fig. 7 Results of (+- .005) simulation

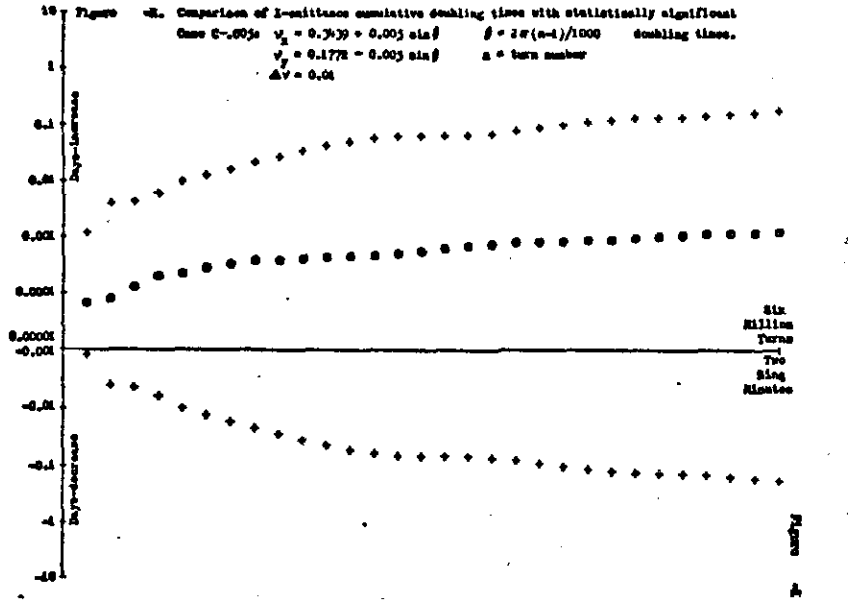

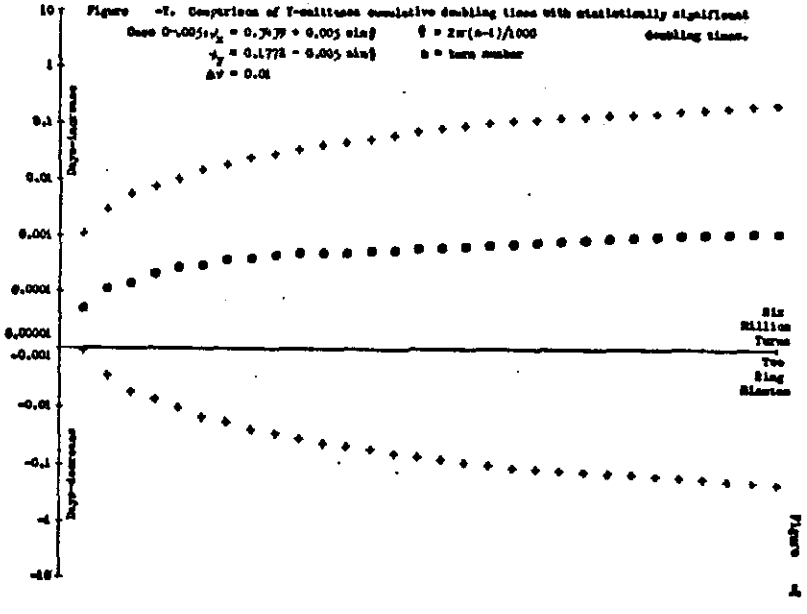

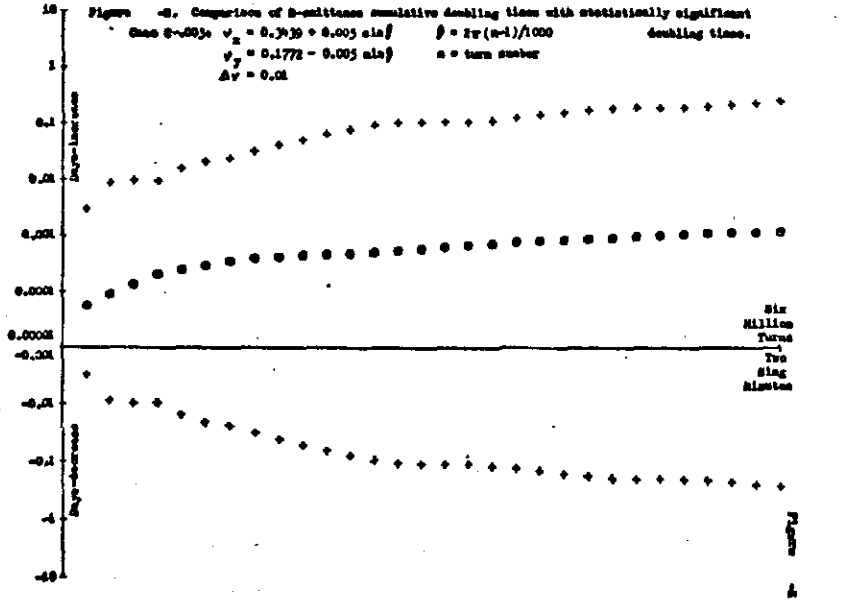

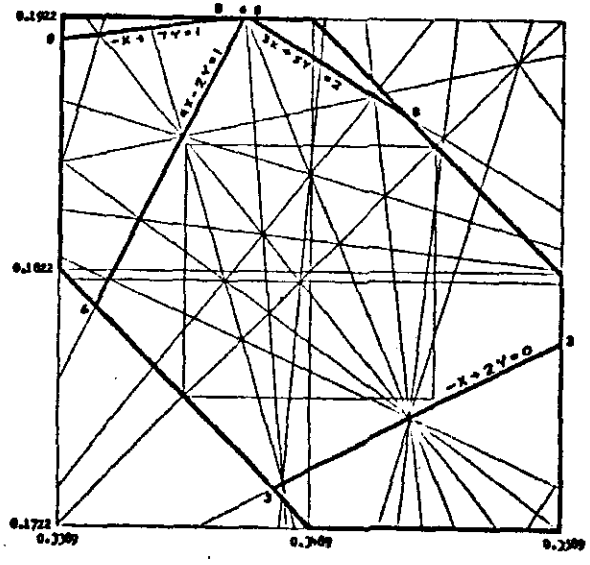

Figure 7

Fig. 8 Results of (+- .010) Simulation

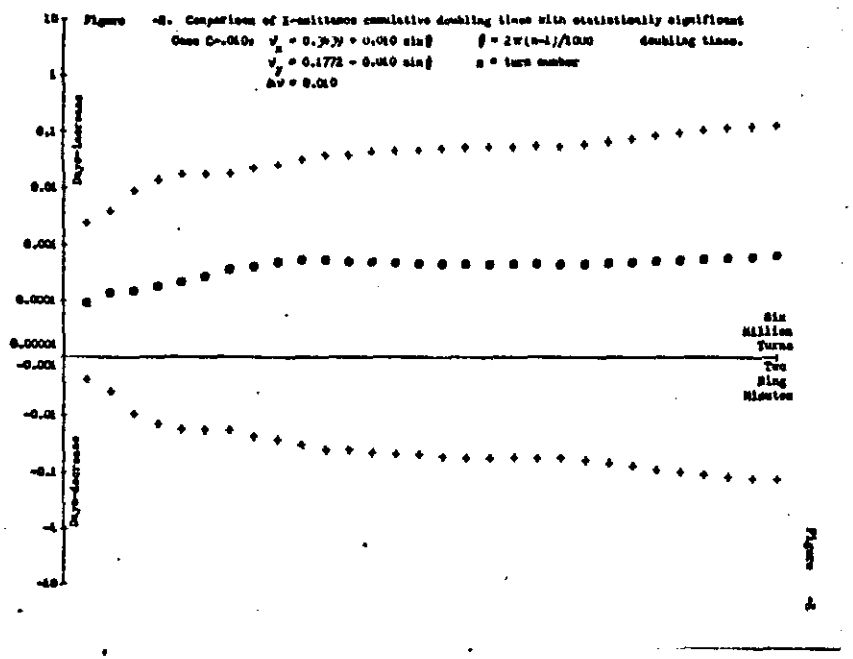

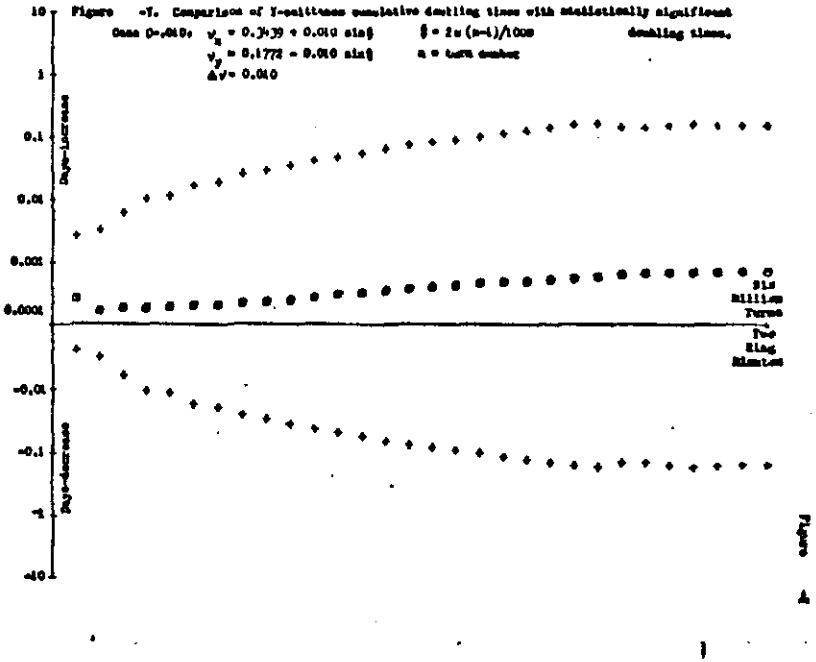

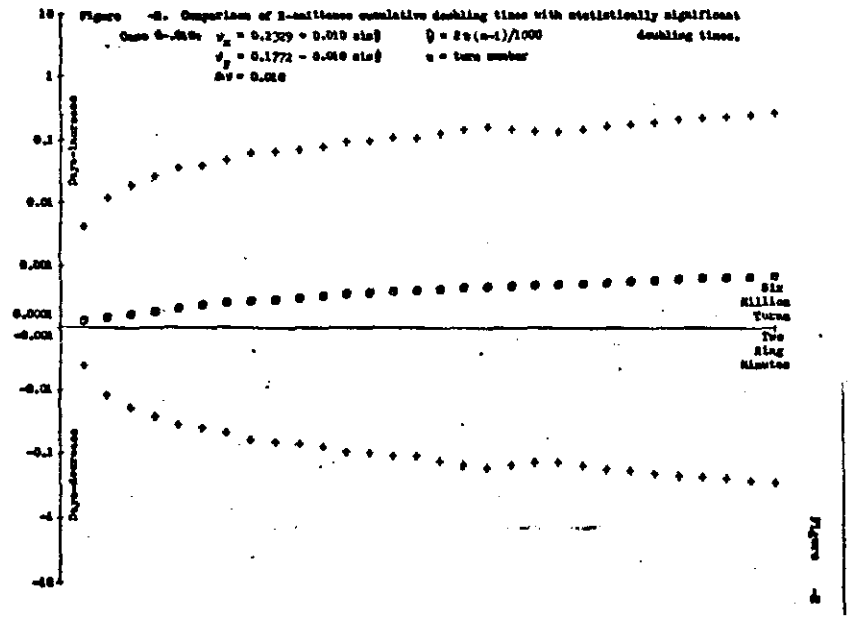

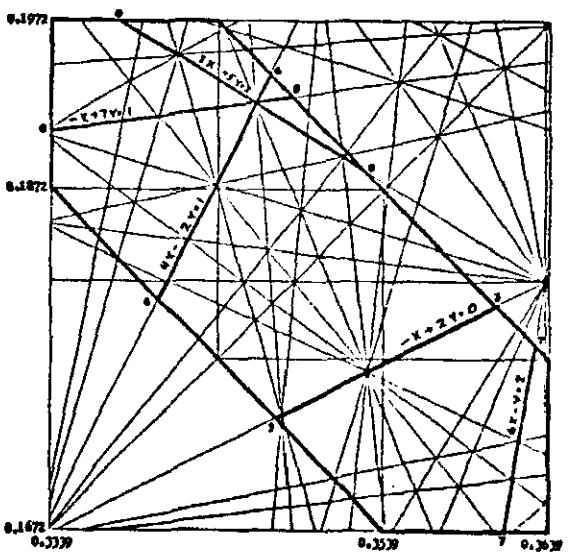

Figure 8

Fig. 9 Area of tune space swept out by

Case C-.005: $\nu_x = 0.3439 + 0.005 \sin\vartheta$ $\quad \vartheta = 2\pi n/1000$

$\nu_y = 0.1772 - 0.005 \sin\vartheta$ $\quad n$ = turn number

$\Delta\nu = 0.01$

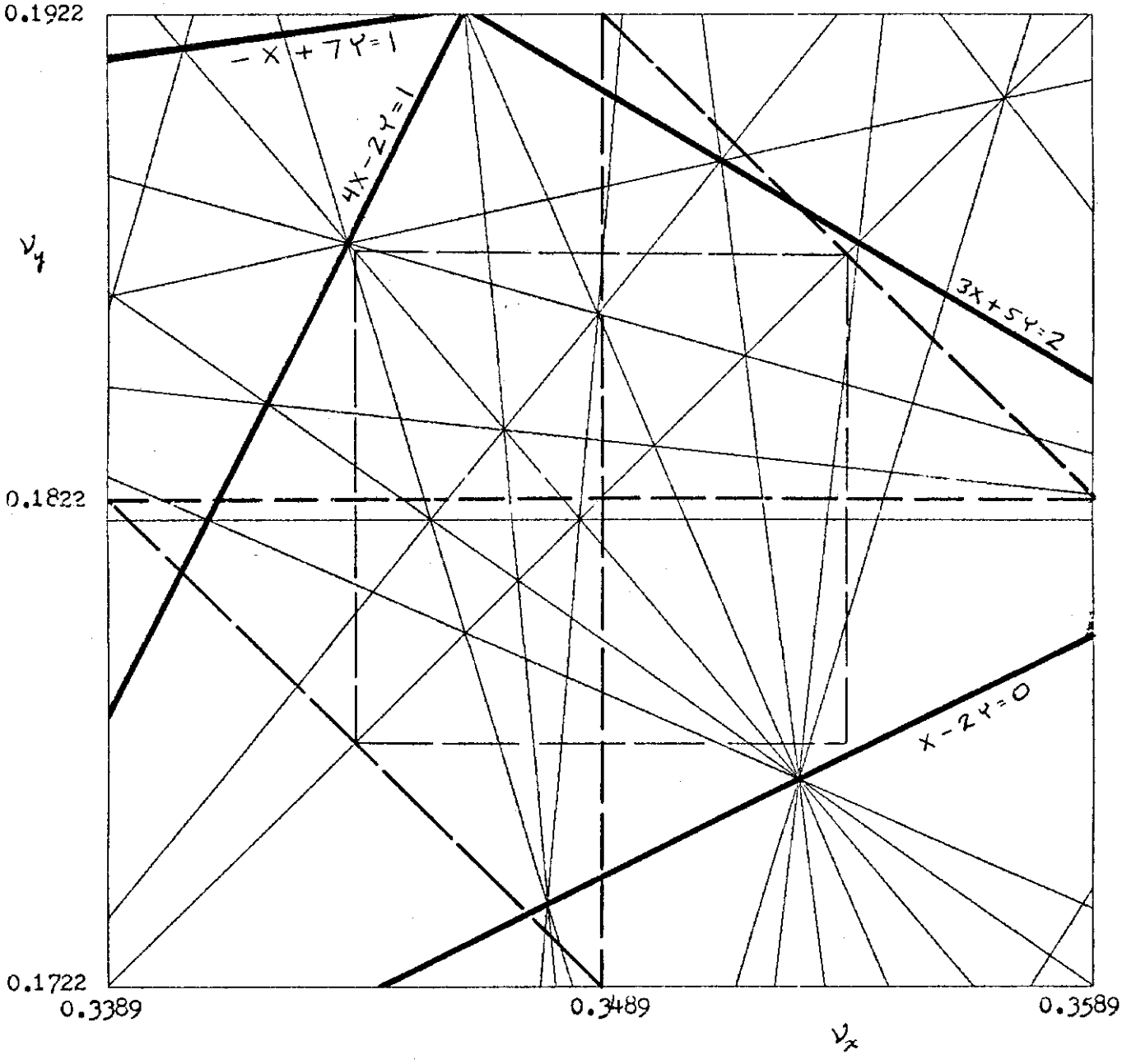

Fig. 10 Tunes averaged over turns 0 to 1000. Case NC-.005
The lower-left corner corresponds with ν_x, ν_y.
The upper-right corner corresponds with $\nu_x + \Delta\nu$, $\nu_y + \Delta\nu$.

Labels: A Reversible and small emittance after 6 million turns.
C Non-reversible and small emittance after 6 million turns.
F Non-reversible and large emittance after 6 million turns.
(F) Also non-reversible for ±0.004 modulation.

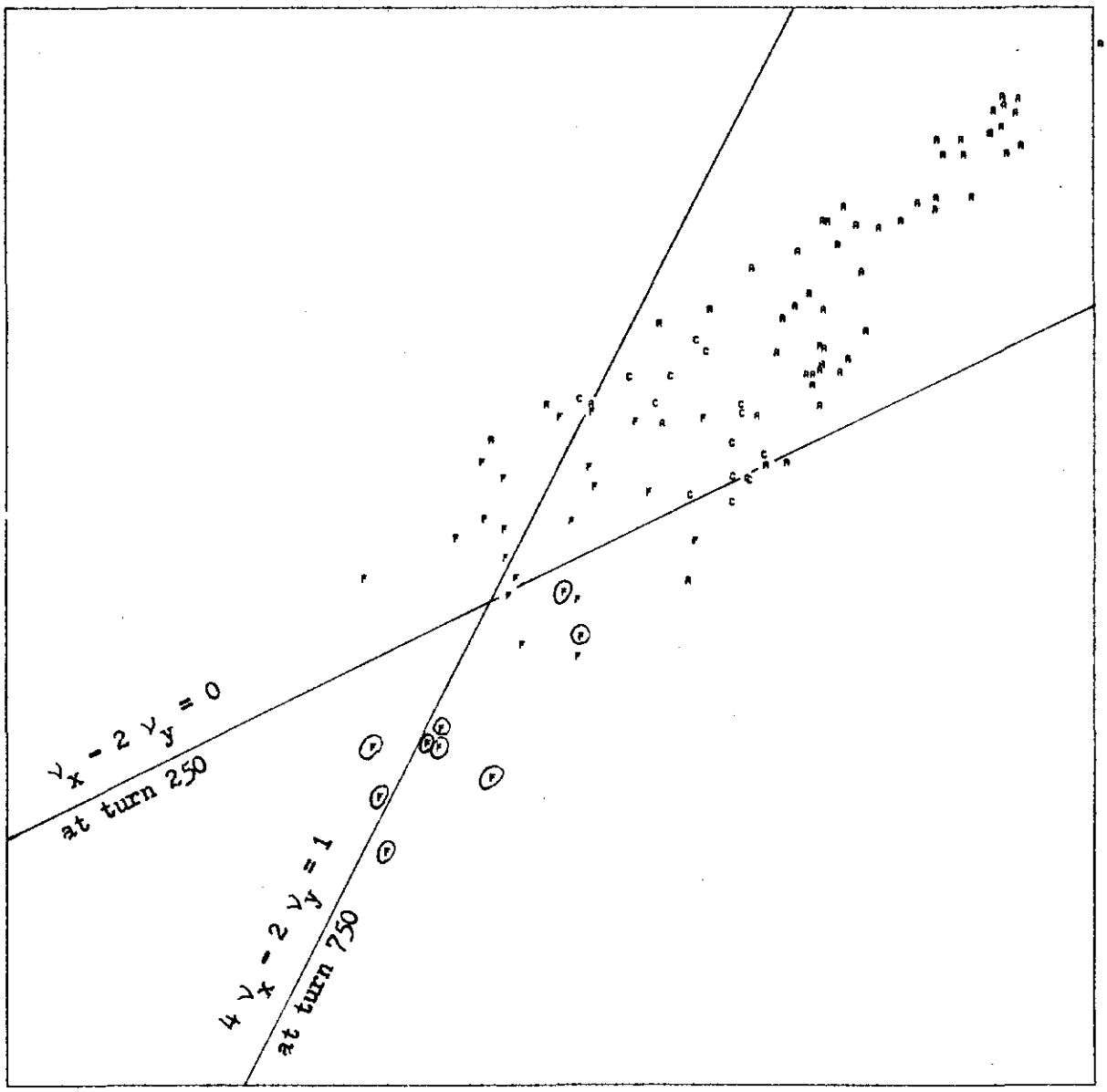

Fig. 11

Figure 11

Individual particle beam-beam tune shift calculation. The total particle tune shift μ_T is calculated by considering motion from the center of one beam-beam kick to the center of the next beam-beam kick.

For the example shown in the first quadrant below, the linear transport $\mu_o = 60^\circ$, $\nu_o = \mu_o/(2\pi) = 0.167$ and the total particle tune shift $\Delta\mu_T = 66^\circ$, $\nu_T = 0.183$ so the beam-beam kicks contribute an additional tune $\Delta\nu_{BB} = 0.016$.

The $\bar{\beta}$ used to scale the vertical dimension is calculated as follows:

$$\bar{\beta} = \begin{cases} 2 & \epsilon_R \leq 0.02 \text{ mm-mrad} \\ \text{linear interpolation} & 0.02 \leq \epsilon_R \leq 0.04 \text{ mm-mrad} \\ \beta_x & 0.04 \leq \epsilon_R \end{cases}$$

where β_x is the matched beta and where $\epsilon_R^2 = \epsilon_X^2 + \epsilon_Y^2$ and where $\epsilon_X = 3(X^2/\beta_x + \beta_x(X')^2)$, $\epsilon_Y = 3(Y^2/\beta_y + \beta_y(Y')^2)$.

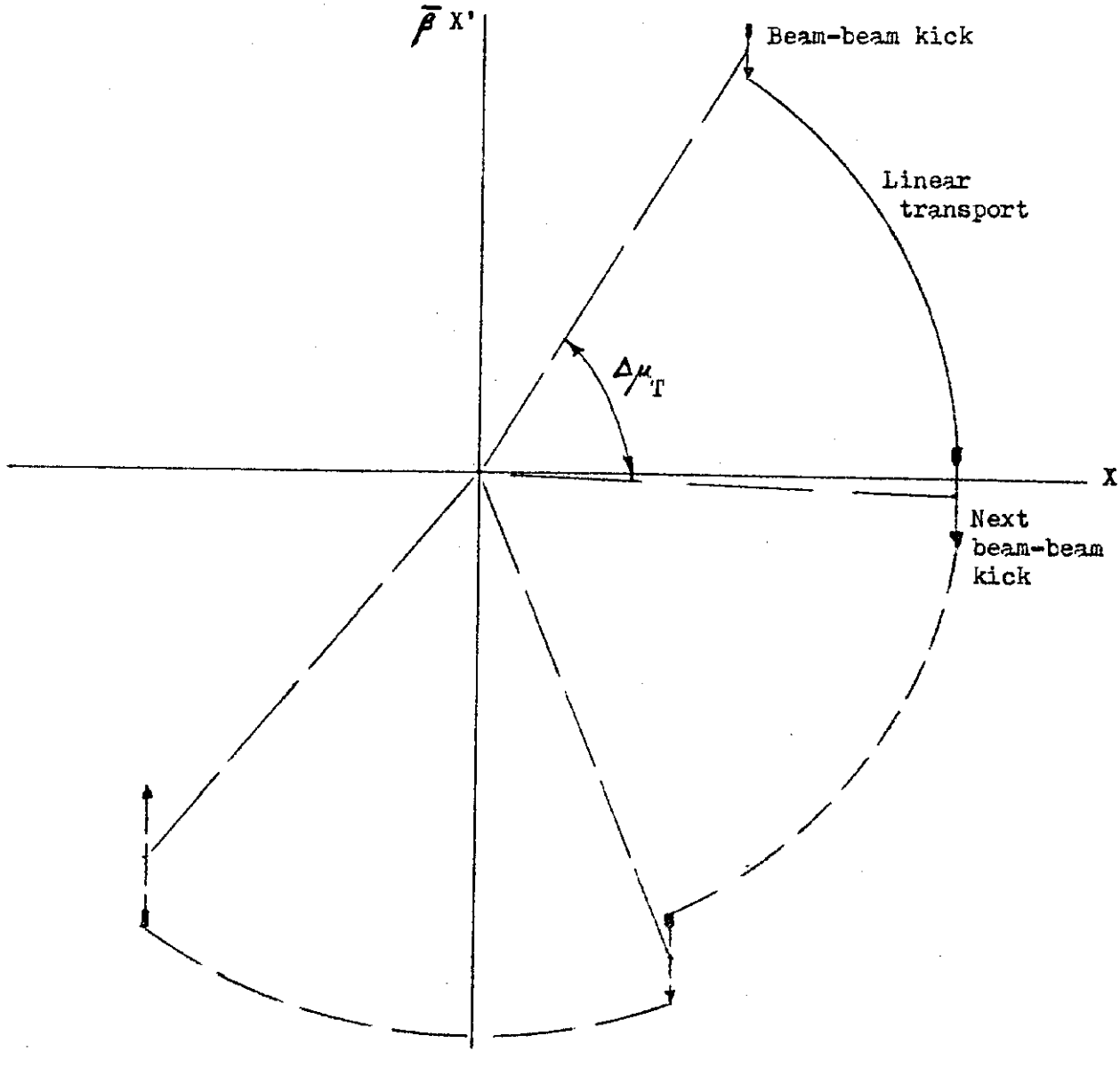

Figure 14 Area of tune space swept out by

Case C+.010: $\nu_x = 0.3439 + 0.010 \sin\theta$ $\quad \theta = 2\pi(n-1)/1000$

$\nu_y = 0.1772 + 0.010 \sin\theta$ $\quad n$ = turn number

$\Delta\nu = 0.010$